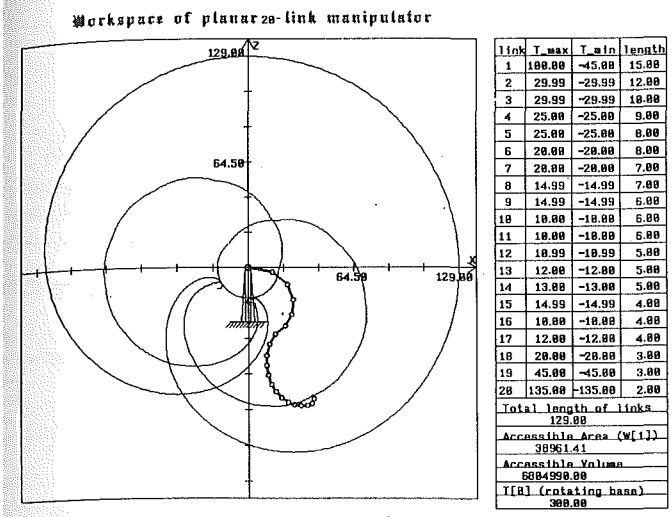

link	T_max	T_min	length
1	180.00	-45.00	15.00
2	29.99	-29.99	12.00
3	29.99	-29.99	10.00
4	25.00	-25.00	9.00
5	25.00	-25.00	8.00
6	20.00	-20.00	8.00
7	20.00	-20.00	7.00
8	14.99	-14.99	7.00
9	14.99	-14.99	6.00
10	10.00	-10.00	6.00
11	10.00	-10.00	5.00
12	10.99	-10.99	5.00
13	12.00	-12.00	5.00
14	13.00	-13.00	5.00
15	14.99	-14.99	4.00
16	10.00	-10.00	4.00
17	12.00	-12.00	4.00
18	20.00	-20.00	3.00
19	45.00	-45.00	3.00
20	135.00	-135.00	2.00

Total length of links
129.00
Accessible Area (W[1])
3896141
Accessible Volume
6804990.00
T[0] (rotating base)
300.00

Fig. 3 The boundary workspace of the 20-link manipulator

the developed angle selection code system is very efficient in plotting workspaces, especially, for a system with a large number of degrees of freedom. Numerical examples were shown for the manipulators with revolute joints and it was shown that the developed algorithm works well for any n-link planar system.

References

1 Gupta, K. C., and Roth, B., 1982, "Design Consideration for Manipulator Workspace," ASME JOURNAL OF MECHANICAL DESIGN, Vol. 104, Oct., pp. 704–711.

2 Kumar, A., and Waldron, K. J., 1981, "The Workspace of a Mechanical Manipulator," ASME JOURNAL OF MECHANICAL DESIGN, Vol. 103, No. 3, July, pp. 665–672.

3 Yang, D. C. H., and Lee, T. W., 1983, "On the Workspace of Mechanical Manipulators," ASME JOURNAL OF MECHANISMS, TRANSMISSIONS, AND AUTOMATION IN DESIGN, Vol. 105, Mar., pp. 62–69.

4 Cwaikala, M., and Lee, T. W., 1985, "Generation and Evaluation of a Manipulator Workspace Based on Optimum Path Search," ASME JOURNAL OF MECHANISMS, TRANSMISSIONS, AND AUTOMATION IN DESIGN, Vol. 107, June, pp. 245–255.

5 Kohli, D., and Spanos, J., 1985, "Workspace Analysis of Mechanical Manipulators using Polynomial Discriminants," ASME JOURNAL OF MECHANISMS, TRANSMISSIONS, AND AUTOMATION IN DESIGN, Vol. 107, June, pp. 209–215.

6 Youm, Y., and Yih, T. C., 1986, "The Kinematic Spaces of Planar n-R Open-Loop System with Rotating Base," ASME Paper, 86-DET-98, *The Design Engineering Conference*, Columbus, OH, October 5–8.

7 Kwon, S. J., 1990, "Self-Collision Avoidance and Workspace Generation for Redundant Manipulators," M.S. thesis, Department of Mechanical Engineering, Pohang Institute of Science & Technology, Dec.

Kinematic Analysis and Design of Articulated Manipulators with Joint Motion Constraints

T. A. Dwarakanath,[1] A. Ghosal,[1] and U. Shrinivasa[1]

For an articulated manipulator with joint rotation constraints, we show that the maximum workspace is not necessarily obtained for equal link lengths but is also determined by the range and mean positions of the joint motions. We present expressions for sectional area, workspace volume, overlap volume and work area in terms of link ratios, mean positions and ranges of joint motion. We present a numerical procedure to obtain the maximum rectangular area that can be embedded in the workspace of an articulated manipulator with joint motion constraints. We demonstrate the use of analytical expressions and the numerical plots in the kinematic design of an articulated manipulator with joint rotation constraints.

[1]Department of Mechanical Engr., Indian Institute of Science, Bangalore—560 012, India.

Contributed by the Mechanisms Committee for publication in the JOURNAL OF MECHANICAL DESIGN. Manuscript received June 1992; Sept. 1993. Associate Technical Editor: G. L. Riuzel.

1 Introduction

The concept of a manipulator workspace and the workspace of the manipulator regional structures has been studied extensively and is well understood (Roth, 1975; Kumar and Waldron, 1980; Hansen et al., 1983; Sugimoto and Duffy, 1981a,b; Tsai and Soni, 1984). Most of the results assume unconstrained joint motions and are not directly applicable to industrial manipulators which usually have limited joint motions. Several researchers have discussed the design of manipulators based on workspace considerations (Tsai and Soni, 1984; Paden, 1986). Again, these are based on the assumption of complete joint rotation. For a manipulator with joint constraints, Rastegar and Deravi (1987) discussed the number of possible configurations as a function of the "overlap" and the "location" of the joint rotation range. Gupta (1986) pointed out the effect of rotation ranges of links on the number of possible configurations. Their treatment is, however, not analytical. Vijaykumar et al. (1985) have discussed the effect of joint limits on workspace and dexterity. However, the design problem is not addressed. In this paper, we present analytical expressions for sectional area, volume, work area and bounding surfaces for an articulated manipulator. We also present a method to choose link lengths, joint ranges and their mean positions to obtain a workspace of given size.

In manipulator applications, such as welding and painting, the total workspace is of less importance. It is more important to know the optimum location and orientation of the part in the workspace since this would allow the operator or task planner to compute how much painting or welding can be done in one setting of the part and the manipulator and thus maximize the use of the manipulator. Very little is known about embedding regular shapes in the workspace. We present an algorithm to obtain the maximum rectangle that can be embedded in the workspace of an articulated manipulator with joint motion constraints.

2 Articulated Manipulators with Joint Constraints

To study the workspace of an articulated manipulator, shown schematically in Fig. 1, we consider the so-called wrist point. Denoting the wrist point by $(x_w, y_w, z_w)^T$, and by using the well known 4×4 matrix transformations (Paul, 1981), we can write

$$(x_w, y_w, z_w) = \{(a_2c_2 + a_3c_{23})c_1, \quad (a_2c_2 + a_3c_{23})s_1, \quad a_2s_2 + a_3s_{23}\} \tag{1}$$

where a_2, a_3 are the link lengths and $c_{(\cdot)}$, $s_{(\cdot)}$ denote cosine and sine of angle $(\cdot)$, respectively. We can eliminate two out of the three θ's from Eq. (1) to obtain equations of the form

$$4a_2^2(x_w^2+y_w^2)c_2^2 - (x_w^2+y_w^2+z_w^2+a_2^2-a_3^2-2a_2s_2z_w)^2 = 0 \tag{2}$$

$$2a_2a_3c_3 + a_2^2 + a_3^2 - (x_w^2+y_w^2+z_w^2) = 0 \tag{3}$$

Equations (2) and (3) represent two families of surfaces but the solid region described by them is the same and is the workspace of the manipulator. The above equation can also be used to study the workspace of a manipulator which has joint motion constraints. If, for example, θ_2 is between $\theta_{2_{\max}}$

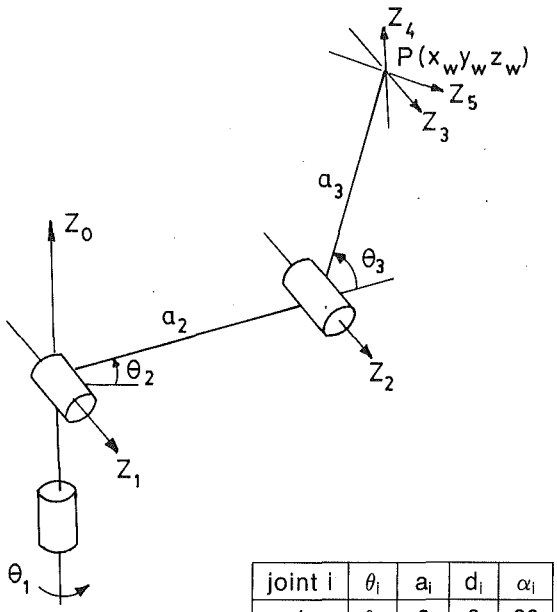

joint i	θ_i	a_i	d_i	α_i
1	θ_1	0	0	90
2	θ_2	a_2	0	0
3	θ_3	a_3	0	0

Fig. 1 An articulated manipulator

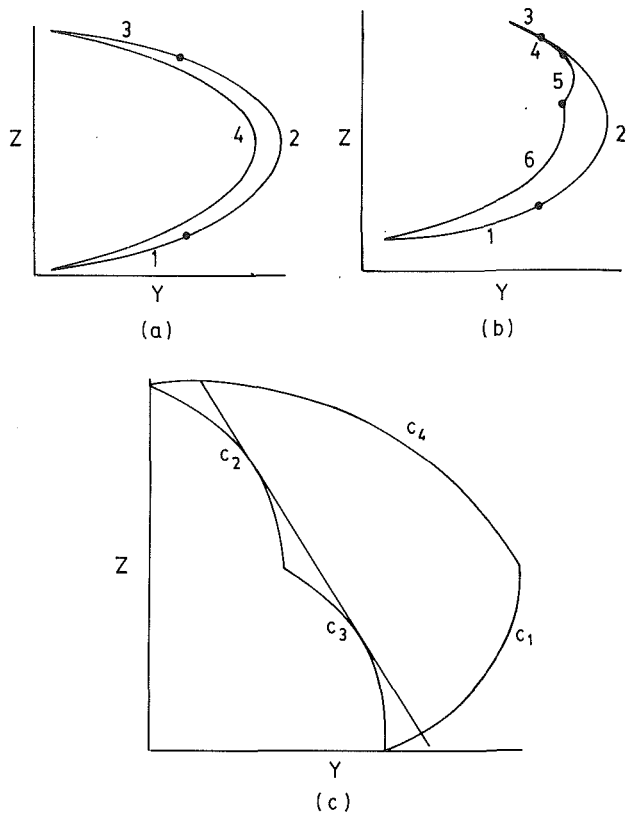

Fig. 2 Sections of workspace in Y_0-Z_0 plane for different cases

and $\theta_{2_{\min}}$, we can find the bounding surfaces by simply substituting $\theta_{2_{\max}}$ and $\theta_{2_{\min}}$ in the above equation.

Instead of using the maximum and minimum values of θ_i ($i=1, 2, 3$), we introduce the mean position and the range of joint motion. The range of the jth joint, θ_{j_r}, and its mean position, θ_{j_m}, in terms of the maximum, $\theta_{j_{\max}}$, and the minimum $\theta_{j_{\min}}$ are given by

$$\theta_{j_r} = \theta_{j_{\max}} - \theta_{j_{\min}}$$
$$\theta_{j_m} = 1/2(\theta_{j_{\max}} + \theta_{j_{\min}}) \quad j=1, 2, 3 \tag{4}$$

The maximum number of bounding surfaces can now be obtained by considering Eqs. (2) and (3). There are three cases.

Case 1: If $\theta_{3_m}=0$, then we get four surfaces—two corresponding to extreme values of θ_2, one corresponding to $\theta_3=0$ and one corresponding to extreme values of θ_3. In Fig. 2(a), we show the four boundary curves in the Y_0-Z_0 plane.

Case 2: If $\theta_{3_m}\neq 0$, but θ_{3_r} contains 0, then we get six surfaces. Figure 2(b) shows the six boundary curves in the Y_0-Z_0 plane.

Case 3: If $\theta_{3_m}\neq 0$ and θ_{3_r} does not contain 0, then we get only 4 surfaces. In Fig. 2(c), we show the four boundary curves in the Y_0-Z_0 plane.

The extreme distance line joining the boundary point and the origin need not intersect the intermediate joint axis. The offset, e_f, defined as the distance between the extreme distance line and the third joint axis is given by $a_2a_3s_3/\sqrt{z_w^2+(x_wc_1+y_ws_1)^2}$. It is clear that only if the range of θ_3 includes zero, then the extreme distance line and the third joint axis intersect.

The number of configurations to reach a generic point in the workspace of an articulated regional structure depends on the range of the angles θ_1 and θ_3. It is clear from Eq. (1) that if θ_{3_r} does not contain 0 or π, then we can get utmost one value of θ_3 and thus one configuration. Whereas if θ_{3_r} contains 0 or π, we will get two configurations. Similarly we will get two values of θ_1 if θ_{1_r} contains π and one value if it does not contain π.

2.1 Boundary Curves. As shown in Fig. 2, there are three cases for the boundary curves. Cases 1 and 2 were observed to yield smaller workspace volume and are discussed in Dwarakanath (1993). The expressions for boundary curves for Case 3 can be easily obtained from Eqs. (2) and (3) by substituting the maximum and minimum θ_i, $i=1, 2, 3$ and then can be written in terms of θ_{i_r} and θ_{i_m} by using Eq. (4) (see Dwarakanath, 1993, for details). The expressions for the intersection points of adjacent curves can be also easily obtained by solving the corresponding equations and are given in Dwarakanath (1993).

2.2 Workspace Volume. The workspace volume is a solid of revolution of the area bounded by the curves C_1 through C_4. The area bounded by the four curves, for Case 3 is given by

$$A = A_1 + A_4 - A_2 - A_3 \tag{5}$$

where A_i, $i=1, \ldots, 4$ is the area under the curve C_i, $i=1, \ldots, 4$, and is obtained by integration between the intersection points. After some algebraic manipulation we can show that A in terms of mean position and range of θ_2 and θ_3 is given as

$$A = 2a_2a_3\theta_{2_r}\sin(\theta_{3_m})\sin(\theta_{3_r}/2) \tag{6}$$

It must be noted that if θ_{3_m} is zero or the range of θ_3 contains zero [see Figs. 2(a) and 2(b)], then the limits of integration and the right-hand side of Eq. (5) have to be altered appropriately. We can observe from Eq. (6) that for a constraint on the link lengths of the form $a_2+a_3=K$ constant and for a given range and mean position of θ_2 and θ_3, the maximum value of A is obtained when $a_2=a_3=K/2$.

Once the sectional area is known, we can obtain the workspace volume as a solid of rotation of the sectional area. The expression of the volume in terms of ranges and mean position of the joint angles is given as

$$V=(1/2)\theta_{1_r}\sin(\theta_{2_r}/2)[2a_2a_3^2(\theta_{3_r}\sin\theta_{2_m}-\sin\theta_{3_r}\sin(2\theta_{3_m}+\theta_{2_m}))$$
$$-8a_2^2a_3\cos\theta_{2_m}\sin\theta_{3_m}\sin(\theta_{3_r}/2)] \quad (7)$$

As can be observed from Eq. (7), the volume is a function of link lengths, mean positions and ranges of joint motions. The maximum volume for $a_2+a_3=K$ constant is obtained by substituting $a_3=K-a_2$ in Eq. (7) and setting $\partial V/\partial a_2=0$. This gives a quadratic equation in a_2 which can be solved as

$$a_2=\{K/3(K_2+4K_3)\}\{K_2+2K_3+\sqrt{(K_2^2+2K_3)^2+12K_3^2}\} \quad (8)$$

where,

$$K_2=\sin\theta_{2_m}-\sin\theta_{3_r}\sin(2\theta_{3_m}+\theta_{2_m}),$$

and

$$K_3=\cos\theta_{2_m}\sin\theta_{3_m}\sin(\theta_{3_r}/2).$$

It may be noted that the negative sign before the square root term gives $a_2<0$ and hence is not used. As can be seen from the above equation, the maximum volume does not occur always for $a_2=a_3=K/2$, but depends on the ranges and mean positions of the joints. In Fig. 3, we plot the normalized volume, $V/[(4/3)\pi(a_2+a_3{}^3]$, as a function of link ratio for various θ_{2_m}. One can easily obtain similar design charts for other joint mean positions and ranges.

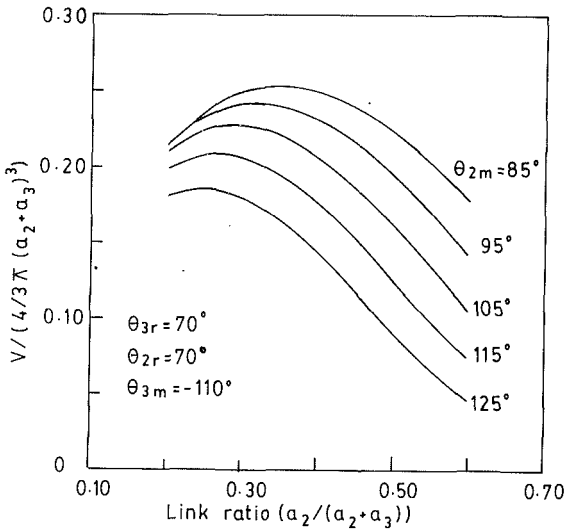

Fig. 3 Workspace volume versus link ratio for varying θ_{2_m}

2.3 Work Area. We call the area determined by the intersection of a plane normal to Y_0–Z_0 plane with the workspace as the work area. In Fig. 2(*c*), the projection of the plane normal to Y_0–Z_0 plane is shown as a straight line $Z_0=mY_0+c$. Since the curves 1 and 4 are convex, the maximum work area is obtained when the above mentioned straight line is either tangent to curves 2 and 3 or to any one of them. A straight line intersecting curves 2 and 3 would give rise to voids in the work area and hence are not of interest. Figure 4 shows the typical work area when the straight line is tangent to curves 2 and 3. The work area consists of two parts, the area A_{w_1} which results from the surface of revolution of curve C_4 about Z_0 axis and the area A_{w_2} which results from the surface of revolution of curve C_1 about Z_0 axis. Area A_{w_1} is the sector of a circle and can be computed in closed form as

$$A_{w_1}=\{\pi/2-\psi\}R^2+R\,O_f\cos(\psi) \quad (9)$$

where R, ψ and O_f are shown in Fig. 4 and their expressions in terms of a_2, a_3 and the minimum and maximum θ_j, $(j=2, 3)$ are given in Dwarakanath (1993).

The expression for area A_{w_2} can be written as

$$A_{w_2}=\int_{\phi_1}^{\phi_2}\sqrt{M_1\cos^2\phi+M_2\sin^2\phi+M_3\cos\phi+M_4\sin\phi+M_5}\,a_3\cos\phi d\phi \quad (10)$$

where the limits of the integration and expressions for M_1 through M_5 are functions of m, c, link lengths, joint ranges and mean positions (see Dwarakanath, 1993). There appears to be no closed form expression for the integral and the area A_{w_2} can be obtained by numerical integration. The total work area is the sum of A_{w_1} and A_{w_2}. The work area depends on the mean positions and the link lengths. It was observed that for a set of mean positions, there exists an optimum link ratio which gave maximum work area.

2.4 Rectangular Area. In many robotic applications such as painting or welding of large surfaces, instead of the complete work area, it is of more interest to find the maximum rectangle that can be embedded inside the workspace or the work area. Due to the difficulty in obtaining closed form expression for A_{w_2}, it is not possible to derive closed form expressions for the area of the maximum rectangle that can be embedded inside the work area. In Appendix A, we present a numerical algorithm to obtain the area of the maximum rectangle that can be embedded inside the work area.

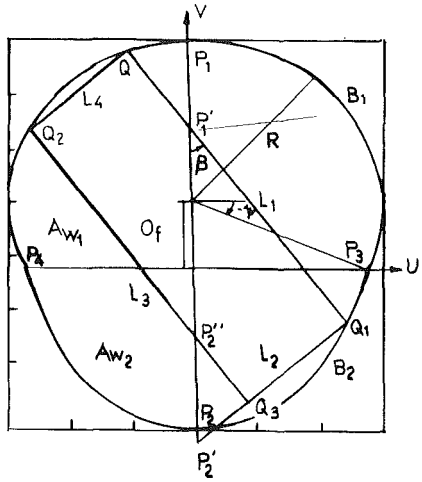

Fig. 4 Rectangle embedded in the work area

It may be mentioned that the area of the rectangle, the orientation, and the aspect ratio depend on link ratio, mean positions and joint rotation ranges. Figure 5 shows the rectangular area as a function of link ratios for various θ_{3_m}. The algorithm can be easily modified to obtain similar design charts for area, orientation, and aspect ratio as a function of other mean positions and joint rotation ranges.

3 Kinematic Design

The results in section 2 can be used for kinematic design of articulated manipulators.

Consider the kinematic design of an articulated manipulator for painting 1.0 m × 1.0 m flat areas. We assume that the joints are hydraulically actuated and the range of rotation are $\theta_{1_r}=2\pi$, $\theta_{2_r}=70$ deg, and $\theta_{3_r}=65$ deg.

The optimum mean position can be found by considering the requirement of embedding the area in the workspace. We

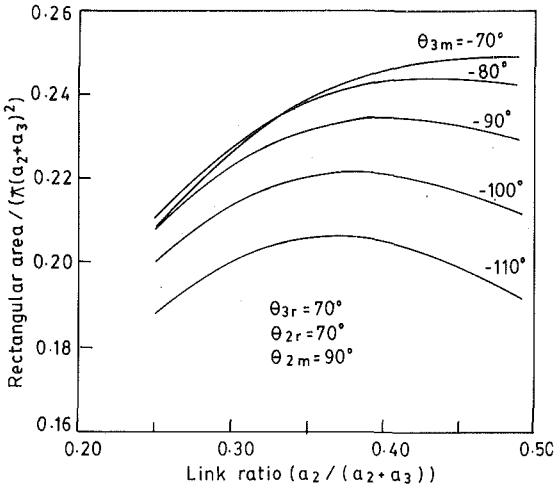

Fig. 5 Rectangular area versus link ratio for varying θ_{3_m}

get $\theta_{2_m} = 90$ deg and $\theta_{3_m} = -60$ deg. The optimum link lengths are $a_2 = 0.66$ m and $a_3 = 0.56$ m. The optimum orientation of the plane containing the area in the workspace is given by 150.70 deg to Y_0 axis.

4 Conclusion

This paper deals with articulated manipulators with joint motion constraints. We have shown that established results known for unconstrained joint motion get modified when joint motions are constrained. We have presented expressions for sectional area, volume in terms of link ratios, mean position and the range of the joint rotation. The concept of a work area has been defined and expression to obtain the work area has been presented. The work area depends on the link ratios, mean position and the joint rotation ranges. We have also presented an algorithm to obtain the maximum rectangular area that can be embedded in the work area. The results show how to obtain the link dimensions and other design parameters like joint ranges and mean positions to meet requirements related to the workspace of the manipulator.

5 Acknowledgment

The first author would like to thank the Council of Scientific and Industrial Research, India, for the support received from grant no. 9/79(334)/91-EMR-I while carrying out this work. The authors would also like to thank the reviewers for their comments.

6 References

Dwarakanath, T. A., 1993, "Towards Optimal Synthesis of Articulated Manipulators with Joint Motion Constraints," Ph.D. Thesis, Dept. of Mechanical Engineering, Indian Institute of Science, Bangalore.

Gupta, K. C., 1986, "On the Nature of Robot Workspace," *Int. Journal of Robotics Research*, Vol. 5, pp. 112–121.

Hansen, J. A., Gupta, K. C., and Kazerounian, S. M. K., 1983, "Generation and Evaluation of the Workspace of a Manipulator," *Int. Journal of Robotics Research*, Vol. 2, pp. 665–672.

Kumar, A., and Waldron, K. J., 1980, "The Dexterous Workspace," ASME paper no. 80 DET-108.

Paden, B. E., 1986, "Kinematics and Control of Robot Manipulators," Ph.D. Thesis, Department of Electrical Engineering, University of California, Berkeley.

Paul, R. P., 1981, *Robot Manipulators: Mathematics, Programming and Control*, The MIT Press, Chapter 3, pp. 65–84, Cambridge.

Rastegar, J., and Deravi, P., 1987, "The Effect of Joint Motion Constraints on the Workspace and Number of Configurations of Manipulators," *Mechanisms and Machine Theory*, Vol. 22, pp. 401–409.

Roth, B., 1975, "Performance Evaluation of Manipulators from a Kinematic Viewpoint," National Bureau of Standards Workshop on Performance Evaluation of Manipulators.

Sugimoto, K., and Duffy, J., 1981, "Determination of Extreme Distances of a Robot Hand—Part 1: A General Theory," ASME JOURNAL OF MECHANICAL DESIGN, Vol. 103, pp. 631–636.

Sugimoto, K., and Duffy, J., 1981, "Determination of Extreme Distances of a Robot Hand—Part 2: Robot Arms With Special Geometry," ASME JOURNAL OF MECHANICAL DESIGN, Vol. 103, pp. 776–783.

Tsai, Y. C., and Soni, A. H., 1984, "The Effect of Link Parameter on the Working Space of General 3R Robot Arms," *Mechanism and Machine Theory*, Vol. 109, pp. 9–16.

Vijaykumar, R., Waldron, K. J., and Tsai, M. J., 1985, "Geometric Optimization of Serial Manipulator Structures for Working Volume and Dexterity," *Int. Journal of Robotics Res.*, Vol. 5, pp. 91–103.

APPENDIX A

The details of the algorithm are given in Dwarakanath (1993). Here we only outline the steps.

(1) Obtain the equations of the curves B_1 through B_4 in the U–V coordinate system (see Fig. 4) from the equations of the boundary curves C_1 through C_4.

(2) Draw line L_1 passing through a point P_1' at an angle β to the axis V (see Fig. 4).

(3) Solve for the intersection point Q_1.

(4) Extend line L_1 to intersect B_1 at Q. Let coordinates of Q be (U_Q, V_Q). Draw the line L_4 perpendicular to L_1 and passing through Q. Solve for the intersection point Q_2 between L_4 and B_1 or B_2.

(5) Draw lines L_2 and L_3 parallel to L_4 and L_1 respectively, and passing through Q_1 and Q_2, respectively. Let L_2 and L_3 intersect V axis at P_2' and P_2'', respectively. Obtain the V coordinates of P_2' and P_2''.

(6) If $|V_{P_2''}| < |V_{P_2'}|$ then the rectangle that can be inscribed in the work area is determined by the points Q_1, Q, Q_2 and the foot of the perpendicular from Q_1 to L_3—else the rectangle that can be inscribed in the work area is determined by the points Q_1, Q, Q_2 and the foot of the perpendicular from Q_2 to L_2.

(7) Find area of the inscribed rectangle from the coordinates of the four points and store result.

(8) Increment β until $\beta \leq \pi/2$ and repeat steps 2 to 7.

(9) Decrement the V intercept of L_1 ($V_{P_1'}$) until zero and repeat steps 1 to 8.

(10) Choose the largest rectangle from those stored in step 7.